Single-Molecule Dynamics of Mechanical Coiled-Coil Unzipping†

Thomas Bornschlögl and Matthias Rief*

Physik Department E22, Technische Universität München, James-Franck-Strasse, D-85748 München, Germany

Received August 1, 2007. In Final Form: September 10, 2007

We use atomic force microscopy (AFM) to mechanically unzip and rezip a double-stranded coiled-coil structure at varying pulling velocities. We find that force-extension traces exhibit hysteresis that grows with increasing pulling velocity. This shows that coiled-coil unzipping and rezipping do not occur in thermal equilibrium on our experimental time scale. We present a nonequilibrium simulation that fully reproduces the hysteresis effects, giving detailed insight into dynamics of coiled-coil folding. Using this model, we find that seed formation is responsible for the hysteresis. The seed consists of four α-helical turns on both strands of the coiled coil. To obtain equilibrium information from our nonequilibrium experiments, we used the Crooks fluctuation theorem (CFT) to calculate the equilibrium free energy of folding for all of the different pulling velocities. The paper presented here lays the groundwork for the study of self-assembly properties of many physiologically relevant coiled-coil structures at the single-molecule level.

Introduction

Many of the processes in living cells rely on the function of proteins. Nevertheless, the formation of 3D functional structures from a nascent polypeptide chain is still a process that is poorly understood. Much effort in recent years has therefore concentrated on understanding the folding of simple model systems. One of the most prominent protein structure to study folding is the coiled coil[1] such as the leucine-zipper region GCN4 of the growth-control transcription factor.[2] Double-stranded coiled coils consist of two α helices that wrap around each other with a pitch of ∼15 nm.[3] Coiled coils exhibit a characteristic heptad repeat[4] consisting of seven amino acids named by letters from a to g. The amino acids at the a and d positions are generally hydrophobic and form the interaction interface of the two coiled-coil helices (Figure 1a).

In the GCN4 leucine zipper, the a and d positions are occupied by an alternating sequence of valines (V) and leucines (L). One position in the leucine zipper breaks this rule and is occupied by a hydrophilic asparagine (N). In this study, we report mechanical single-molecule experiments with a triple-GCN4-like leucine zipper (LZ26)[5] schematically shown in Figure 1b. Although mechanical unfolding under equilibrium conditions has been studied in an earlier paper,[5] in the present study we investigate the unzipping and rezipping of LZ26 at various experimental velocities in nonequilibrium. We present a non-equilibrium model that is able to describe in detail the observed hysteresis between unzipping and rezipping. Moreover, using the Crooks fluctuation theorem[6] we can extract the equilibrium folding free energy from nonequilibrium experiments. Beyond protein folding model systems, coiled coils occur in various mechanically active proteins in a cell ranging from molecular motors and cytoskeletal proteins to synaptic fusion proteins. Understanding the mechanics of the GCN4 model system will likely provide valuable information for understanding those physiologically important structures.

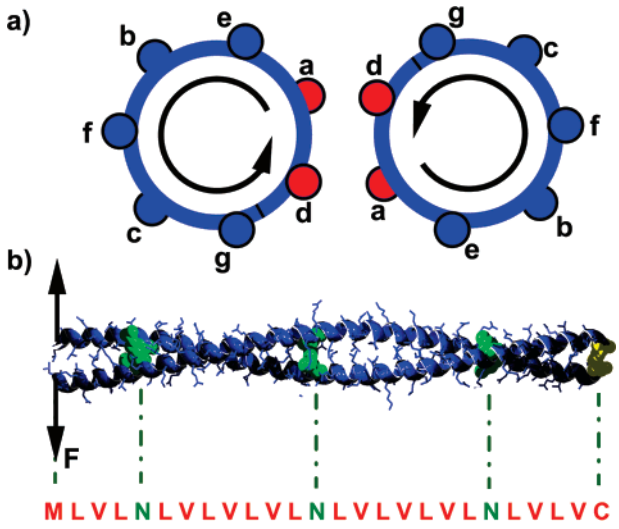

Figure 1. (a) Schematic drawing of a cross section of a double-stranded, parallel coiled coil viewed from the c terminus. Shown is one heptad repeat (approximately two turns) with amino acids named by letters from a to g. (b) Schematic structure of the used LZ26 zipper, where the sequence specifies every α-helical turn by the amino acid at an a or d position.

Experimental Section

Coiled-Coil Unzipping at High Resolution. To unzip and rezip single coiled-coil molecules with atomic force microscopy, we designed an artificial protein by adding a coiled-coil strand to the c-terminal end of the actin cross-linker protein ddFLN(1-5). Homodimerization of the coiled coil leads to the molecule that is schematically shown in Figure 2a, which is covalently connected by a c-terminal cysteine bridge.

The ddFLN(1-5) molecule acts as matrix protein to which a surface and an AFM tip can bind and which propagates the applied force to both n-terminal ends of the coiled coil. Moreover, it provides a clear single-molecule fingerprint in the force-extension traces as shown in Figure 2a. In the sawtooth-like force-extension pattern, one can clearly identify six peaks that correspond to individual unfolding events, always leading to the same increase in extension, before the molecule detaches from the surface or cantilever tip.

† Part of the Molecular and Surface Forces special issue.

* To whom correspondence should be addressed. E-mail: mrief@ph.tum.de.

(1) Mason, J. M.; Arndt, K. M. *ChemBioChem* **2004**, *5*, 170−176.
(2) O'Shea, E. K.; Klemm, J. D.; Kim, P. S.; Alber, T. *Science* **1991**, *254*, 539−544.
(3) Phillips, G. N., Jr. *Proteins* **1992**, *14*, 425−429.
(4) Gruber, M.; Lupas, A. N. *Trends Biochem. Sci.* **2003**, *28*, 679−685.
(5) Bornschlögl, T.; Rief, M. *Phys. Rev. Lett.* **2006**, *96*, 118102.
(6) Crooks, G. E. *Phys Rev E* **1999**, *60*, 2721−2726.

10.1021/la7023567 CCC: $40.75
Published on Web 11/01/2007

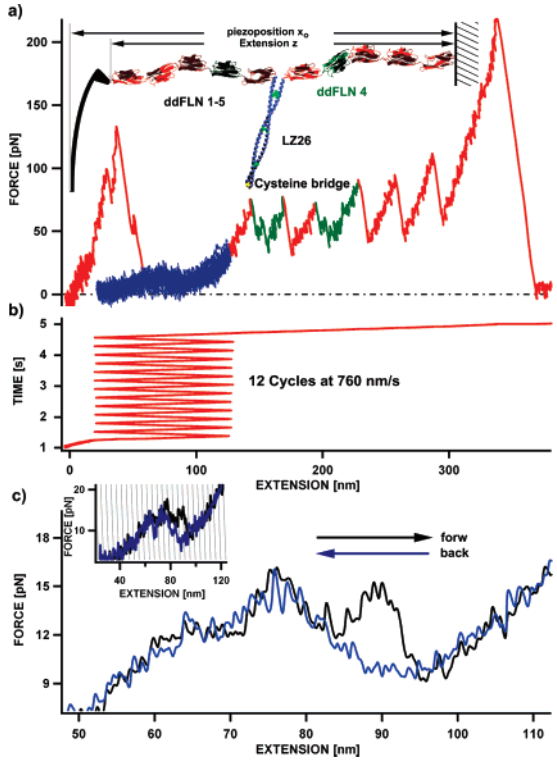

Figure 2. (a) Force-extension trace of the investigated coiled-coil structure with added ddFLN(1-5) matrix proteins.[5] The protein construct is schematically shown in the inset. (b) Time vs extension trace showing 12 alternating approach and retraction cycles of the cantilever tip to the surface, followed by complete retraction of the tip. (c) Averaged force-extension trace of LZ26 unzipping and rezipping from four different molecules. The averaged force-extension trace of the 12 cycles obtained with only one coiled-coil molecule is shown in the inset.

The force-extension behavior of ddFLN(1-5) has been well investigated.[7,8] It has been shown that domain 4 (ddFLN 4) unfolds via a stable intermediate (green in Figure 2a). Thus, the observation of two ddFLN 4 unfolding events in a force-extension curve ensures that the attachment of the molecule to both the surface and cantilever tip has occurred in the desired manner: distal to both ddFLN4 domains. Such force curves always contain the force signal of coiled-coil unzipping at the beginning of the force-extension traces (blue in Figure 2a) at forces below 20 pN. In this regime, force fluctuations of the cantilever caused by thermal noise nearly mask the unzipping signal. To improve the signal-to-noise ratio, we average multiple force-extension traces of the same coiled-coil molecule. To this end, after the initial tip−sample contact of 1 s to allow protein adsorption to the cantilever tip, we consecutively retract and approach the surface with respect to the cantilever tip with constant velocity v (Figure 2b). We stop the reapproaching ∼30 nm before the cantilever tip reaches the surface to avoid binding of additional proteins to the cantilever tip, and we retract only up to extensions where the unfolding of further matrix domains is unlikely. After the last cycle, we completely retract the tip, which leads to full unfolding of the matrix protein as discussed above. In this manner, we obtain several force-extension traces of the unzipping and rezipping coiled coil, which we average separately by taking the average of data points within 1 nm piezo position intervals. The inset in Figure 2c shows the outcome of the averaging process for the unzipping (black) and rezipping (blue) force-extension traces (intervals are schematically drawn in gray). The signal-to-noise ratio of the traces gained from a single coiled-coil molecule can be further improved by applying the averaging procedure for approximately four preaveraged force-extension traces from other molecules with similar elastic polypeptide spacers. The length of the elastic polypeptide spacers is determined by fitting the wormlike chain interpolation formula[9] with variable contour length to the first and last rising slopes of the coiled-coil unzipping data. The final averaged forward and backward force-extension traces taken at a velocity of 760 nm/s are shown in Figure 2c.

Theoretical Basis

Equilibrium Theory. In thermal equilibrium, the probability of finding the system in a certain accessible state has a Boltzmann distribution. To describe the equilibrium unfolding of LZ26, we adapted a model originally developed by Bockelmann et al.[10,11] to describe DNA unzipping. The accessible states for our experimental system are parametrized by the extension of the unfolded polypeptide spacer (z), the degree of cantilever bending ($x_0 - z$), and the number of unzipped coiled-coil turns (j). We can then calculate the thermal average of an observable (e.g., force at given piezo position x_0) by summation over all accessible states j and z:

$$\langle F(x_0)\rangle = \frac{\sum_{j,z} F(j, z, x_0) e^{-E_{TOT}(j,z,x_0)/k_B T}}{\sum_{j,z} e^{-E_{TOT}(j,z,x_0)/k_B T}}$$

The energy E_{TOT} in the Boltzmann factor is explained in more detail in the following paragraph.

Energy Landscape Contributions. The total energy of the system E_{TOT} is given by three contributing parts that arise from the bending of the cantilever, $E_{LEV} = k_C/2(x_0 - z)^2$; the stretching of the elastic polypeptide chain with contour length $L(j)$, $E_{WLC} = \int_0^z F_{WLC}(L(j), z')\,dz'$; and the energy needed to unzip j individual coiled-coil turns, $E_{CC}(j) = \sum_{\nu=1}^{j} E_{turn}(\nu)$. The spring constant of our cantilever force probe is $k_C = 6$ pN/nm. To describe the force response F_{WLC} of the elastic polypeptide chain consisting of a serial arrangement of unfolded and folded ddFLN domains and the partially unfolded coiled coil, we take the interpolation formula introduced by Bustamante et al.[9] using a persistence length of $A = 0.7$ nm. The total energy is then given by the sum of the contributing parts $E_{TOT} = E_{LEV} + E_{WLC} + E_{CC}$. It is important to note that only E_{CC} contains unknown fit parameters but both E_{LEV} and E_{WLC} are known. A representative energy landscape for E_{TOT} versus opened turns at zero force is shown in Figure 3b. At zero force, there are no energy contributions from the lever E_{LEV} or from the elastic polymer E_{WLC}, thus the energy landscape represents only the contributions from E_{CC}. If a force is applied to the system by retracting the cantilever tip from the surface, then the contributions from E_{LEV} and E_{WLC} become nonzero and change the relative energy barriers between the different states as shown in Figure 3c. Also, the positions of the local energy minima can change because of the elastic energy contributions (position 2 in Figure 3c).

Monte Carlo Simulation. To reproduce the experimental conditions exactly, we stretched a virtual elastic polypeptide spacer with contour length $L_{[i]}$ and velocity v starting with the coiled coil in the totally zipped state [1]. For every time step, this leads to an increasing extension and thus to a change in the total energy landscape as explained in the Energy Landscape

(7) Schwaiger, I.; Kardinal, A.; Schleicher, M.; Noegel, A. A.; Rief, M. *Nat. Struct. Mol. Biol.* **2004**, *11*, 81−85.
(8) Schlierf, M.; Rief, M. *J. Mol. Biol.* **2005**, *354*, 497−503.
(9) Bustamante, C.; Marko, J. F.; Siggia, E. D.; Smith, S. *Science* **1994**, *265*, 1599−1600.
(10) Bockelmann, U.; Essevaz-Roulet, B.; Heslot, F. *Phys. Rev. Lett.* **1997**, *79*, 4489−4492.
(11) Bockelmann, U.; Thomen, P.; Essevaz-Roulet, B.; Viasnoff, V.; Heslot, F. *Biophys. J.* **2002**, *82*, 1537−1553.

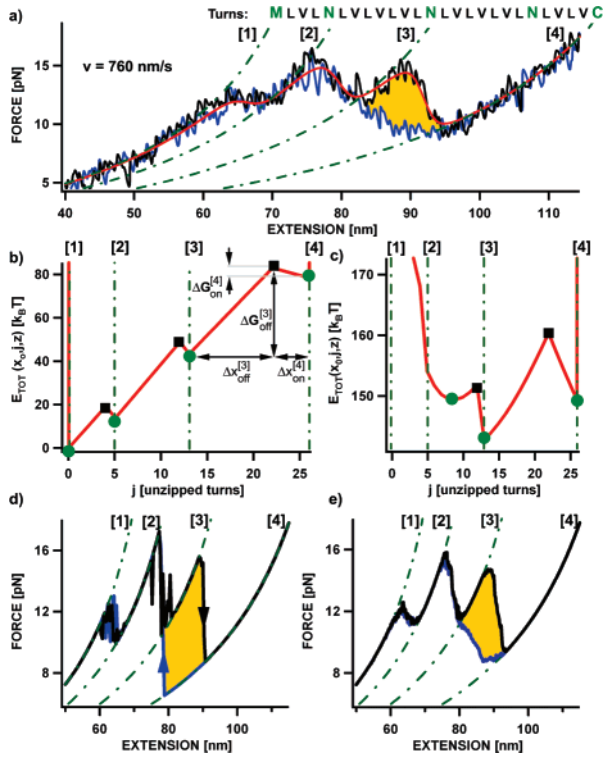

Figure 3. (a) Force-extension trace of the LZ26 coiled coil, where the hysteresis between unzipping (black) and rezipping (blue) traces is shaded in orange. Overlaid is the theoretical force-extension behavior calculated with equilibrium theory (red trace). (b) Energy landscape for coiled-coil unzipping at zero applied force. The parameters are $\Delta x_{off}^{[3]} = 9 \pm 1$ [turns], $\Delta x_{on}^{[4]} = 4 \pm 1$ [turns], $\Delta G_{off}^{[3]} = 39.8 \pm 1.5 k_B T$, and $\Delta G_{on}^{[4]} = -4.5 \pm 0.8 k_B T$. (c) Tilted energy landscape due to applied force. (d) Single forward and backward force-extension traces calculated by the nonequilibrium simulation. (e) Average of 30 different simulated force-extension traces. Hysteresis is again shaded in orange.

Contributions section. For every time step, we extract from E_{TOT} the actual barrier heights $\Delta G_{on/off}^{[i]}$ that are separating the actual state [i] from the neighboring ones (Figure 3b,c). According to $k_{on/off}^{[i]} = k_0 \exp(\Delta G_{on/off}^{[i]}/k_B T)$, we calculate the actual rates that provide us with the probabilities for rezipping/unzipping transitions by $dP_{on/off}^{[i]} = k_{on/off}^{[i]}(x_0, j, z)\, dt$. A computer-generated random number then decides if a transition occurs. If a transition occurs, we change the actual state of the system as well as the contour length of the elastic polypeptide spacer $L_{[i]}$. Please note that no further zipping is possible if the zipper is in state [1] ($\Delta G_{on}^{[1]} = \infty$) and no further unzipping is possible if the zipper is in state [4] ($\Delta G_{off}^{[4]} = \infty$). The actual force at every time step can be calculated by using the wormlike chain interpolation formula.[9]

Results and Discussion

The simplest approach for modeling the unzipping of a coiled coil is the assumption of true equilibrium throughout the unzipping process. This assumption was made in our previous study.[5] This equilibrium model follows earlier work by Bockelmann et al.[10,11] and is described in the Theoretical Basis section. In brief, for every position of the cantilever base, the partition function for the whole mechanical system is calculated, including energetic contributions of the bending cantilever and polypeptide spacers as well as the energy costs to open individual turns of the coiled coil. This equilibrium model is very successful in describing many features of the unzipping traces, as can be seen in Figure 3a (red trace). However, rezipping experiments consistently exhibited hysteresis (orange area in Figure 3a), indicating that the process is not in true equilibrium.

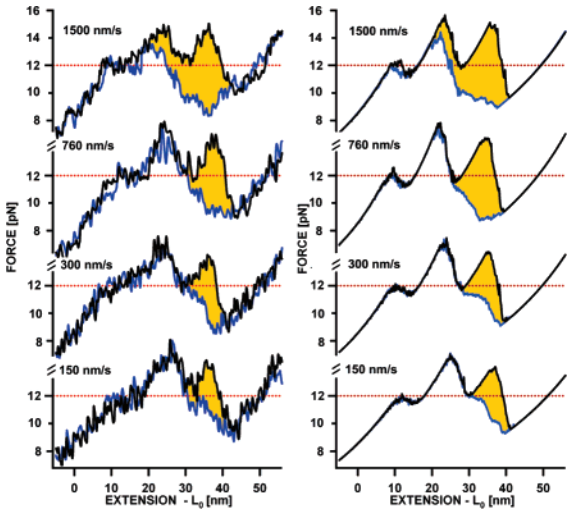

Figure 4. (a) Unzipping and rezipping force-extension data at four different pulling velocities. (b) Unzipping and rezipping force-extension traces calculated by the nonequilibrium simulation. For better comparison of the traces, we subtracted the extension of the individual polypeptide spacer at 12 pN (L_0) from the data.

We therefore set out to perform speed-dependent measurements of coiled-coil unzipping and rezipping that should allow us to describe this process in a nonequilibrium framework providing access to the dynamics. In Figure 4a, we show four averaged unzipping and rezipping traces of LZ26 obtained at four different pulling velocities (150, 300, 760, and 1500 nm/s). For details of the protein construction and averaging procedures, see the Experimental Section. Consistent with the expectation of a nonequilibrium process, we find that the hysteresis (marked as orange) between unzipping (black) and rezipping (blue) traces grows with pulling velocity.

To develop a kinetic nonequilibrium model able to reproduce these dynamic features of the unzipping and rezipping process, we describe the energy landscape of the leucine zipper by four energetic minima that constitute four states ([1]−[4] in Figure 3) of the leucine zipper on its way from the zipped to the unzipped configuration. The state positions of those minima in the leucine zipper sequence can be determined by fitting WLC traces with variable contour lengths to the rising slopes of the unzipping traces (green dashed lines in Figure 3a). Interestingly, the position of the minima coincides with the position of asparagines (N) in leucine zipper sequence[5] (Figure 3a). The kinetic scheme for the LZ26 coiled-coil unzipping and rezipping can hence be described as

$$[1] \underset{k_{on}^{[2]}}{\overset{k_{off}^{[1]}}{\rightleftharpoons}} [2] \underset{k_{on}^{[3]}}{\overset{k_{off}^{[2]}}{\rightleftharpoons}} [3] \underset{k_{on}^{[4]}}{\overset{k_{off}^{[3]}}{\rightleftharpoons}} [4] \qquad (1)$$

where $k_{on/off}^{[i]}(x_0, z, j)$ denotes the rezipping and unzipping rates between the various states. Note that the rates will depend on an externally applied force because force affects the energy barriers as detailed in the Theoretical Basis section. With knowledge of the force dependence of the kinetic scheme (eq 1), we can obtain the underlying energy landscape. $k_{on/off}^{[i]}(x_0, z, j)$ can readily be calculated from energy barrier heights according to $k_{on/off}^{[i]} = k_0 \exp(\Delta G_{on/off}^{[i]}/k_B T)$ where $\Delta G_{on/off}^{[i]}(x_0, z, j)$ represents the barrier heights between states i and i − 1 for the on rate and between states i and i + 1 for the off

rate, respectively. We chose $k_0 = 1 \times 10^7\ s^{-1}$, consistent with literature values.[12,13] Figure 3d shows an example for a nonequilibrium simulation of a single unzipping and rezipping cycle of the LZ26 coiled coil. (See also the Monte Carlo Simulation section.) The black trace represents unzipping, and the blue trace corresponds to rezipping of the coiled coil. The traces are filtered with a 2 kHz low-pass filter to represent the time resolution of our cantilever probe. The apparent noise in the simulated traces results from rapid flipping between states that cannot be resolved in detail because of the limited bandwidth. We averaged 30 simulated traces (Figure 3e) in a manner similar to that used for the experimental data. The averaged traces now allow a direct adaptation of simulation parameters to match experimental data.

By adapting the barrier positions and heights for the transitions to the values given in Figure 3b, we were able to fully reproduce the distinct hysteresis pattern of coiled-coil unzipping and rezipping at four different pulling velocities (Figure 4b). It is important to note that, in the experiment, hysteresis can be observed only in the transition between [3] and [4] (Figure 3a). Hence, transitions between all other states must occur quickly compared to the experimental time scale under all conditions. The respective energy barriers $\Delta G_{on}^{[2],[3]}$ had to be chosen ($<8.5 k_B T$) so that transitions between those states are always faster than the experimental time scale (>2 kHz) at all pulling velocities. Hence, the only determinant of hysteresis is the energy barrier between states [3] and [4], which represents seed formation for coiled-coil zipping. Our nonequilibrium model now allows for closer insight into the kinetics and structure of this seed formation which limits the folding speed of leucine zippers.[14,15] Interestingly, the value we find for $k_{on}^{[4]} = 1 \times 10^5\ s^{-1}$ in the absence of force for seed formation agrees very well with solution studies of a c-terminal cross-linked leucine zipper.[16] Moreover, we find a value of $\Delta x_{on}^{[4]} = 4$ turns corresponding to 14 amino acids of each strand that have to lock into the right position before downhill folding toward the fully folded state can proceed. The size of the seed agrees surprisingly well with various solution studies[17,18] where values ranging from 3 to 5 turns have been reported. Our data also shows that nucleation starts at the cross-linked c-terminal end when the coiled coil is mechanically rezipped. The good agreement between our mechanical experiments and solution data to rates measured by chemical denaturation argues for one folding path starting with the nucleation at the tethered end[16] in both types of experiments.

Coiled-coil formation offers an ideal system to take advantage of fluctuation theorems relating equilibrium and nonequilibrium properties of a thermodynamic system.[19−23] A recent experimental approach used the Crooks fluctuation theorem[6] (CFT) to extract the equilibrium free energies for RNA folding from nonequilibrium single-molecule data.[24] From the CFT (see equation below), it follows that the equilibrium value for the folding free energy ΔG_0 is given by the intersection of probability distributions for nonequilibrium unfolding $P_{off}^{[3]}(E)$ and refolding $P_{on}^{[4]}(-E)$ plotted on a free-energy axis.

$$\frac{P_{off}^{[3]}(E)}{P_{on}^{[4]}(-E)} = \exp\left(\frac{E - \Delta G_0}{k_B T}\right)$$

As shown above, all but the last transition along the folding/unfolding pathway from states [1]↔...↔[4] occur in equilibrium. An analysis using the CFT can now be used to calculate the equilibrium free energy for the transition $[3] \underset{k_{on}^{[4]}}{\overset{k_{off}^{[3]}}{\rightleftharpoons}} [4]$ even though our measurements of this last transition occur in nonequilibrium. At first sight, it may seem that applying the CFT requires the direct detection and compilation of unzipping and rezipping events from individual curves. However, in our experiments we rely on an averaging procedure of up to 240 individual unzipping and rezipping traces to achieve the required force resolution as described in the Experimental Section. Thus, an averaged curve obtained from individual events can already be regarded as a representation of a probability distribution. We can therefore

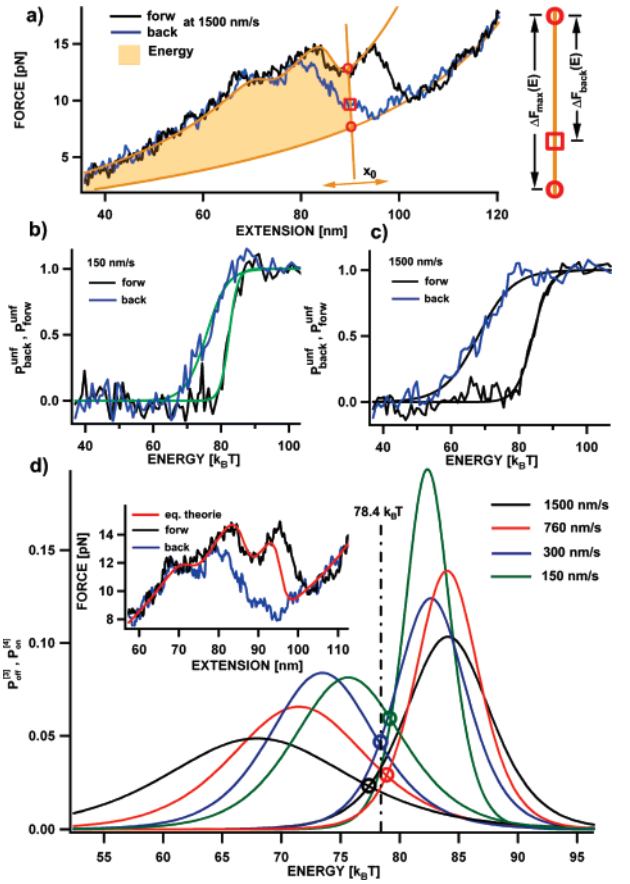

Figure 5. (a) Reconstruction of the folding probability connected to a certain energy (shaded orange). (b) Probability functions to find an unfolded coiled coil dependent on the energy at pulling velocities of 150 nm/s and (c) 1500 nm/s. (d) Probability distributions for unzipping and rezipping as a function of energy at four different pulling velocities. The inset shows the force-extension traces collected at 1500 nm/s overlaid with the theoretical equilibrium trace using the equilibrium energy of 78.4 k_BT.

(12) Lapidus, L. J.; Eaton, W. A.; Hofrichter, J. *Proc. Natl. Acad. Sci. U.S.A.* **2000**, *97*, 7220−7225.
(13) Yang, W. Y.; Gruebele, M. *Nature* **2003**, *423*, 193−197.
(14) Steinmetz, M. O.; Jelesarov, I.; Matousek, W. M.; Honnappa, S.; Jahnke, W.; Missimer, J. H.; Frank, S.; Alexandrescu, A. T.; Kammerer, R. A. *Proc. Natl. Acad. Sci. U.S.A.* **2007**, *104*, 7062−7067.
(15) Kammerer, R. A.; Schulthess, T.; Landwehr, R.; Lustig, A.; Engel, J.; Aebi, U.; Steinmetz, M. O. *Proc. Natl. Acad. Sci. U.S.A.* **1998**, *95*, 13419−13424.
(16) Krantz, B. A.; Sosnick, T. R. *Nat. Struct. Biol.* **2001**, *8*, 1042−1047.
(17) Zitzewitz, J. A.; Ibarra-Molero, B.; Fishel, D. R.; Terry, K. L.; Matthews, C. R. *J. Mol. Biol.* **2000**, *296*, 1105−1116.
(18) Moran, L. B.; Schneider, J. P.; Kentsis, A.; Reddy, G. A.; Sosnick, T. R. *Proc. Natl. Acad. Sci. U.S.A.* **1999**, *96*, 10699−10704.
(19) Evans, D. J.; Cohen, E. G.; Morriss, G. P. *Phys. Rev. Lett.* **1993**, *71*, 2401−2404.
(20) Gallavotti, G.; Cohen, E. G. *Phys. Rev. Lett.* **1995**, *74*, 2694−2697.
(21) Ciliberto, S.; Laroche, C. *J. Phys. IV* **1998**, *8(Proc 6)*, 215−220.
(22) Jarzynski, C. *Phys. Rev. Lett.* **1997**, *78*, 2690−2693.
(23) Seifert, U. *Phys. Rev. Lett.* **2005**, *95*, 040602.
(24) Collin, D.; Ritort, F.; Jarzynski, C.; Smith, S. B.; Tinoco, I., Jr.; Bustamante, C. *Nature* **2005**, *437*, 231−234.

extract the probability distributions for the work performed during refolding and unfolding directly from the averaged rezipping and unzipping traces, respectively. This procedure is exemplified in Figure 5.

The blue trace in Figure 5a is the average of 240 single refolding traces of LZ26. The lower orange trace corresponds to a force curve if the zipper permanently stays in the unfolded state [4]. The upper orange trace is the force curve expected if the zipper can go through all equilibrium conformations [1]−[3] but cannot be unfolded to state [4]. The red square marks the experimental average force of refolding at a given piezo position x_0. If in all 240 single curves refolding had not occurred, then the square would lie on top of the lower red cycle marking the unfolded state [4]. Instead, if in all traces at this position refolding had occurred, then the red square would lie on the upper red circle. Hence, the fraction of events where refolding from [4] to [3] has not taken place at this position can be readily calculated by $P_{\mathrm{back}}^{\mathrm{unf}}(E) = \Delta F_{\mathrm{back}}/\Delta F_{\mathrm{max}}$. The energy that corresponds to the work performed if refolding occurs is then given by the shaded area in Figure 5a. This calculation can now be performed for all positions on both the zipping (blue) and unzipping traces (black). The obtained probability functions for two different pulling velocities are shown in Figure 5b for 150 nm/s and Figure 5c for 1500 nm/s. The probability distributions can now be calculated by the derivation of those probability functions. To reduce the noise that naturally is associated with derivatives, we fitted the probability functions using a Fermi function (green and black in Figure 5b,c.). The resulting probability distribution for unzipping and rezipping as a function of work at the four measured velocities is given in Figure 5d. It becomes immediately obvious that the distributions for folding and unfolding are further apart at higher pulling velocities (black) as compared to those at low pulling velocities (green). This merely reflects that the system shifts toward equilibrium with decreasing velocity. According to the CFT, the equilibrium free energy should be given by the intersection of the folding and the unfolding distribution at every given velocity[24] (colored circles). The agreement at all velocities is striking, and a value of $(78.4 \pm 4)k_{\mathrm{B}}T$ can be extracted for the equilibrium free energy of folding for the LZ26 construct.

Even though the nonequilibrium model with the underlying energy landscape of Figure 3b was originally developed to describe deviations from equilibrium, it necessarily also must contain information about the equilibrium free energy of LZ26 (rightmost green dot in Figure 3b). Comparing this value ($79.2k_{\mathrm{B}}T$) to the value obtained from the Crooks fluctuation theorem ($78.4k_{\mathrm{B}}T$) shows excellent agreement. Hence, the CFT independently validates this important parameter of our nonequilibrium model.

Moreover, this value for the equilibrium free energy can now be used to refine our original equilibrium model. Whereas in the original model (Figure 3a, red trace) we assumed that the entire unzipping process is in equilibrium, we can now calculate by how much the last unzipping step from state [3] to [4] is off equilibrium. In the inset of Figure 5d, the equilibrium curve (red trace) using the total unzipping free energy from the CFT is superimposed with the unzipping and rezipping trace at 1500 nm/s. In contrast to the original assumption (red curve in Figure 3a),[5] the equilibrium curve now lies in between the black and the blue curve as expected from an experiment not performed at equilibrium.

Conclusions

We show that mechanical unzipping experiments of coiled-coil structures exhibit complex behavior comprising slow seed formation, resulting in speed-dependent hysteresis followed by rapid equilibrium folding into the fully folded structure. Using a nonequilibrium model to describe the seed formation kinetics under load, we could get information about the unloaded kinetics of seed formation as well as the size of the seed. In addition, using the Crooks fluctuation theorem, we could extract the equilibrium free energy for zipper folding even though all data were obtained under nonequilibrium conditions. The analysis presented here forms the basis for the interpretation of future experiments with biologically important coiled-coil structures.

Acknowledgment. We thank G. Woehlke, M. Schliwa, H. Dietz, and E. Wasner for helpful discussions. Financial support of the German Excellence Initiative via the "Nanosystems Initiative Munich (NIM)" is gratefully acknowledged.

LA7023567